12. B. Kramarsky, N. H. Sarkar, D. H. Moore, *Proc. Natl. Acad. Sci. U.S.A.* **68**, 1603 (1971); M. A. Gonda, D. L. Fine, M. Gregg, *Arch. Virol.* **56**, 297 (1977).
13. R. E. Benveniste *et al.*, in preparation.
14. V. S. Kalyanaraman, M. G. Sarngadharan, B. Poiesz, F. W. Ruscetti, R. C. Gallo, *J. Virol.* **38**, 906 (1981).
15. E. Hefti, J. Ip, W. E. Giddens, Jr., S. Panem, *Virology* **127**, 309 (1983).
16. S. Panem, personal communication.
17. R. E. Benveniste *et al.*, *Biochem. Biophys. Res. Commun.* **81**, 1363 (1978).
18. R. E. Benveniste and G. J. Todaro, *Proc. Natl. Acad. Sci. U.S.A.* **74**, 4557 (1977).
19. W. Drohan, D. Colcher, G. Schochetman, J. Schlom, *J. Virol.* **23**, 36 (1977).
20. M. D. Daniel *et al.*, *Science* **223**, 602 (1984).
21. P. A. Marx *et al.*, *ibid.*, p. 1083.
22. T. G. Kawakami *et al.*, *Nature (London) New Biol.* **235**, 170 (1972); T. G. Kawakami, G. V. Kollias, Jr., C. Holmberg, *Int. J. Cancer* **25**, 641 (1980).
23. M. M. Lieber *et al.*, *Proc. Natl. Acad. Sci. U.S.A.* **72**, 2315 (1975).
24. L. O. Arthur, B. W. Altrock, G. Schochetman, *Virology* **110**, 270 (1981).
25. Supported in part with federal funds from the Department of Health and Human Services under contracts N01-CO-23910 with Program Resources, Inc., and N01-CO-23909 with Litton Bionetics, Inc.; and NIH grants RR00166 and RR01203 from the Division of Research Resources. We thank B. Kramarsky for electron microscopy, W. B. Knott, R. W. Hill, T. C. Shaffer, and S. A. Vargo for technical assistance, and D.A. Huffer for clerical assistance.
* To whom requests for reprints should be sent.

10 February 1984; accepted 12 March 1984

Spatially Nonuniform Changes in Intracellular Calcium Ion Concentrations

Abstract. *The spatial variation of changes in intracellular calcium ions were studied with a one-dimensional scanning microphotometer. Changes in intracellular calcium were measured with a metallochromic dye, arsenazo III. Both the magnitude and the kinetics of changes in calcium were dramatically different in different regions of a cell. In* Limulus *ventral photoreceptors the maximum change was probably restricted to the rhabdomeric lobe.*

Changes in the concentration of calcium ions in the cytosol $[Ca^{2+}]_i$ are important for the control of physiological and metabolic processes in a wide variety of cells. Changes in $[Ca^{2+}]_i$ can arise from calcium ions that enter through the plasma membrane or that are released from intracellular stores. Any change in $[Ca^{2+}]_i$ might be restricted spatially by diffusion barriers, sequestration mechanisms, or active removal. Such restrictions to the spread of changes in $[Ca^{2+}]_i$ have been indicated by the apparent nonuniformity of Ca^{2+} buffering capacity in the soma of a molluscan neuron (*1*) and of salivary gland cells in larval insects (*2*) and by the radial nonuniformity of changes in $[Ca^{2+}]_i$ demonstrated in squid giant axons (*3*).

We examined the spatial nonuniformity of changes in $[Ca^{2+}]_i$ in single cells. We studied *Limulus* ventral photoreceptors because these cells use Ca^{2+} as an intracellular messenger to signal changes in sensitivity to light (*4*). Our results indicate that $[Ca^{2+}]_i$ does not change uniformly throughout the photoreceptor cell and that measurements of the magnitude and kinetics of changes in $[Ca^{2+}]_i$ can be seriously distorted by spatial nonuniformity.

We used a metallochromic dye, arsenazo III, to measure changes in $[Ca^{2+}]_i$. In most previous studies the absorption of intracellular dye was measured through an aperture that restricts the measuring light to that passing through an entire segment of a tubular cell (*5*) or much or all of the cell soma (*6*). Changes in dye absorption were presumed to indicate the magnitude and kinetics of changes in $[Ca^{2+}]_i$ that could be correlated with physiological events. Results obtained by this method are difficult to interpret because the distribution of changes in

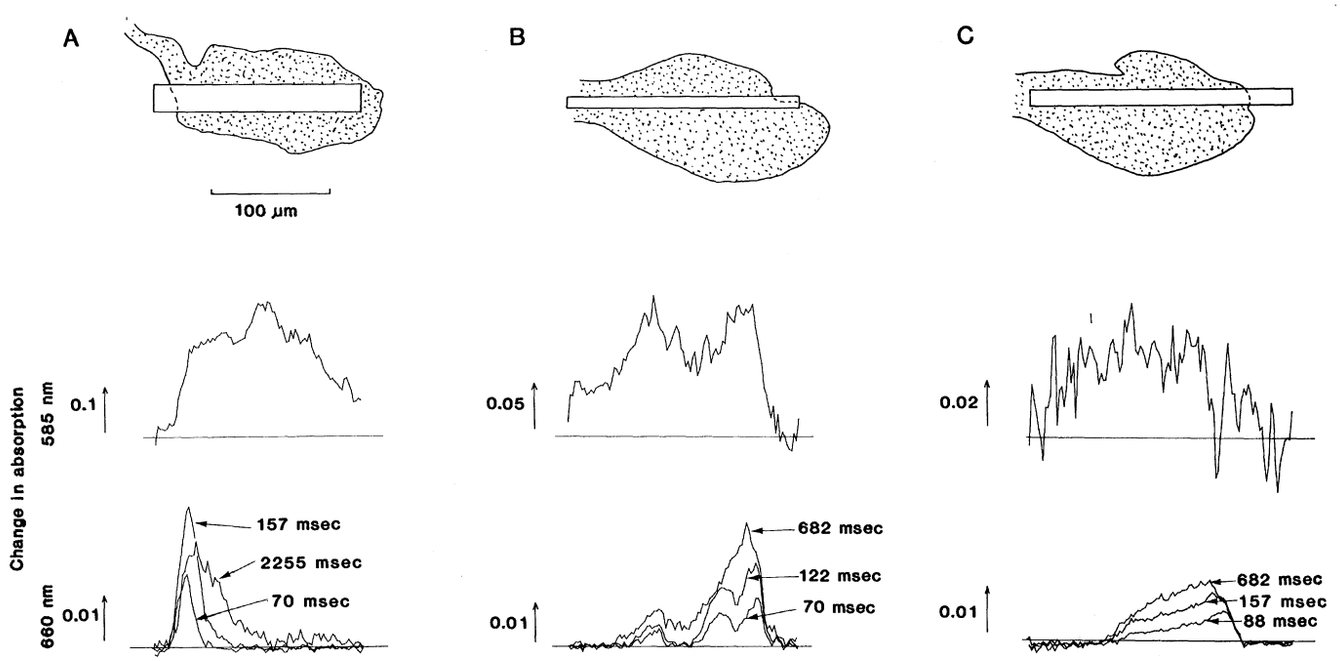

Fig. 1. (A to C) Examples of the spatial distribution of stimulus-induced changes in the absorption of intracellular arsenazo III. (Top) Outlines of the cell and measuring slit as traced from micrographs taken through the measuring optics. In each outline the axon exited from the cell body toward the left. (Middle) Changes in absorption, measured at the isosbestic wavelength (585 nm), as a function of distance across the cell. (Bottom) Changes in absorption, measured at 660 nm, as a function of distance across the cell. The times indicated are the times of the beginning of each scan; scan duration was 18 msec. (A) The change in absorption was localized to the end of the cell nearest the axon. This pattern was observed in two cells. Note that the peak change in absorption at 660 nm rose and fell as a function of time and that at the longest time the absorption profile became broadened. In 13 other cells the change in absorption at 660 nm was localized to the end of the cell opposite the axon. (B) Absorption at 660 nm increased at more than one region of the cell. This is most evident in the 70-msec trace. This pattern was observed in five cells. (C) The change in absorption at 660 nm was broadly distributed across the cell. This pattern was observed in one cell.

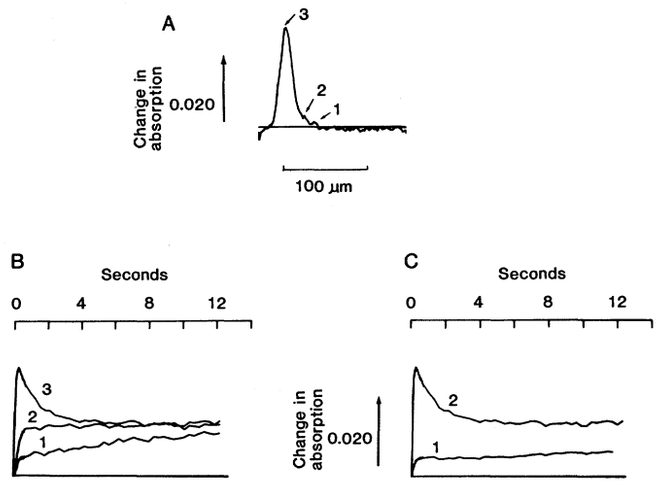

Fig. 2. Kinetics of stimulus-induced changes in $[Ca^{2+}]_i$ in different regions of a *Limulus* ventral photoreceptor cell. (A) Spatial distribution of the change in arsenazo III absorption at 660 nm measured 700 msec after a light stimulus had been given to the photoreceptor. The change in absorption was localized to one end of the cell. (B) Time course of the change in arsenazo III absorption at 660 nm measured at three different points. In trace 3 absorption rose and fell more quickly at the peak of the spatial distribution [point 3 in (A)] than at other points in the cell. In most previous studies light passing through the entire cell containing arsenazo III was focused onto the detector, that is, an average change in absorption was measured for the entire cell. (C) (Trace 1) Average change in absorption for the entire cell. Absorption was calculated after first summing the intensities measured at each position along the length of the cell at each time. (Trace 2) Absorption change at the peak of the spatial distribution [identical to trace 3 in (B)]. The average change in trace 1 lacks the transient aspect of the kinetics of the absorption change seen at the peak of the spatial distribution (trace 2). Note also that the magnitude of the simulated average change in absorption (trace 1) is considerably smaller than the absorption change at the peak of the spatial distribution. Therefore both the magnitude and the kinetics of the change in intracellular Ca^{2+} inferred from arsenazo III measurements depend on the spatial distribution of the arsenazo III signals.

$[Ca^{2+}]_i$ throughout the cell volume is either unknown or can be estimated only roughly (*7, 8*). The technique we used can reveal spatial nonuniformity of changes in $[Ca^{2+}]_i$ in a single cell with a spatial resolution of about 2 μm and a time scale of tens of milliseconds.

Purified arsenazo III was injected into single ventral photoreceptor cells of *Limulus* (*9*) through micropipettes. Membrane voltage and changes in optical transmission were recorded simultaneously (*10*). To detect spatial differences in optical transmission across a single cell, the preparation was uniformly illuminated and the image of that cell was projected onto a linear diode array (Princeton Applied Research). The diode elements were scanned sequentially to produce a linear (one-dimensional) profile of optical transmission across the cell. Optical absorption of the dye was computed from profiles of optical transmission (*11*). The middle traces in Fig. 1 are profiles of the optical absorption of intracellular arsenazo III in single *Limulus* ventral photoreceptors.

After excitation of a *Limulus* ventral photoreceptor cell $[Ca^{2+}]_i$ [as detected by aequorin (*12*) or arsenazo III (*10*)] increased and then declined (Fig. 1A). The increase in $[Ca^{2+}]_i$ was not uniform across the cell; the initial increase was confined to the end of the cell nearest the axon. As $[Ca^{2+}]_i$ began to decline the spatial distribution of the increased $[Ca^{2+}]_i$ broadened. These findings indicate that $[Ca^{2+}]_i$ was diffusing away from the region in which it was released into the cytosol and was simultaneously being removed from the cytosol (*13*). In this cell the change in $[Ca^{2+}]_i$ remained restricted to one end of the cell; that is, diffusion of $[Ca^{2+}]_i$ was restricted in the cytosol by some unknown combination of binding sites, tortuousity of diffusion paths, and removal mechanisms. In other cells the increase in $[Ca^{2+}]_i$ that followed excitation occurred in more than one region (Fig. 1B) or occurred broadly along the cell's length (Fig. 1C).

The kinetics of the stimulus-induced increase in $[Ca^{2+}]_i$ differed with location. This finding is illustrated in Fig. 2. The change in absorption of arsenazo III was recorded as a function of time at several places across the cell. At the place where the change in dye absorption was maximal, both the increase and the decrease were more rapid than at other locations (Fig. 2B). For comparison, we simulated a measurement made across the whole cell by averaging the changes in absorption over the entire length of the diode array covered by the image of the cell. The time course of this spatial average (trace 1 in Fig. 2C) was very different from that of the signal measured at the place of maximum change (trace 2 in Fig. 2C) (*14*). Thus, measurement of the optical changes of a metallochromic dye averaged across a large region of a single cell may distort the magnitude and kinetics of the changes in intracellular ion concentrations. In each case where values of these quantities are important, some estimate of the spatial distribution of optical changes of the dye ought to be made.

Localization of the light-induced increase in $[Ca^{2+}]_i$ in one or more well-defined regions of *Limulus* ventral photoreceptors suggests a correlation with the known anatomy. In many cells there is a rhabdomeric lobe distal to the axon; in other cells there may be two or more lobes bearing rhabdoms, and occasionally rhabdoms are found along much of the cell surface (*15, 16*). The rhabdom contains rhodopsin and is the region of the cell in which the excitatory events are initiated (*16*). Light-induced modulation of the excitatory events is localized to the region where light has been absorbed (*17*), and a light-induced increase in $[Ca^{2+}]_i$ is a component of the light adaptation mechanism (*3*). Thus, the observation of local light-induced increases in $[Ca^{2+}]_i$ is consistent with a function of $[Ca^{2+}]_i$ in *Limulus* ventral photoreceptors.

H. H. HARARY
J. E. BROWN
Department of Physiology and Biophysics, State University of New York, Stony Brook 11794, and *Marine Biological Laboratory, Woods Hole, Massachusetts 02543*

References and Notes

1. D. Tillotson and A. L. F. Gorman, *Nature (London)* **286**, 816 (1980).
2. B. Rose and W. R. Loewenstein, *Science* **190**, 1204 (1975).
3. L. J. Mullins and J. Requeña, *J. Gen. Physiol.* **74**, 393 (1979).
4. J. Lisman and J. E. Brown *ibid.* **59**, 701 (1972); J. E. Brown, *Biophys. Struct. Mech.* **3**, 141 (1977).
5. Examples include the use of (i) arsenazo III in squid giant axons [J. E. Brown *et al.*, *Biophys. J.* **15**, 1155 (1975); R. DiPolo *et al.*, *J. Gen. Physiol.* **67**, 433 (1976)] and in frog skeletal muscle) [L. Kovacs, E. Rios, M. F. Schneider, *Nature (London)* **279**, 391 (1977); R. Miledi, I. Parker, G. Schalow, *Proc. R. Soc. London Ser. B* **198**, 201 (1977); P. Palade and J. Vergara, *J. Gen. Physiol.* **79**, 101 (1982); S. M. Baylor, W. K. Chandler, M. W. Marshall, *J. Physiol. (London)* **331**, 139 (1982); (ii) dichlorophosphonazo III in squid giant axons [J. E. Brown *et al.*, *Biophys. J.* **15**, 1155 (1975)] and in frog skeletal muscle [S. M. Baylor, W. K. Chandler, M. W. Marshall, *J. Physiol. (London)* **331**, 139 (1982)]; and (iii) antipyrylazo III in squid giant axons [F. J. Brinley, T. Tiffert, A. Scarpa, *J. Gen. Physiol.* **72**, 101 (1978)] and in frog skeletal muscle [P. Palade and J. Vergara, *J. Gen. Physiol.* **79**, 679 (1982); S. M. Baylor, W. K. Chandler, M. W. Marshall, *J. Physiol. (London)* **331**, 139 (1982)].
6. Examples include the use of arsenazo III in *Limulus* ventral photoreceptors [J. E. Brown, P. K. Brown, L. H. Pinto, *J. Physiol. (London)* **267**, 299 (1977)] and in molluscan neurons [A. L.

F. Gorman and M. V. Thomas, *ibid.* **275**, 357 (1977); Z. Ahmed and J. A. Connor, *ibid.* **286**, 61 (1979)].
7. S. J. Smith and R. S. Zucker, *J. Physiol. (London)* **300**, 167 (1980).
8. J. A. Connor and G. Nikolakopoulou, *Lect. Math. Life Sci.* **15**, 79 (1982).
9. R. Demoll, *Zool. Jahrb. Abt. Anat. Ontog. Tiere* **38**, 443 (1914); A. W. Clark, R. Millecchia, A. Mauro, *J. Gen. Physiol.* **54**, 289 (1969).
10. J. E. Brown *et al.* (*6*). The light-induced increase in absorption at 660 nm of arsenazo III inside *Limulus* ventral photoreceptors is largely if not entirely due to an increase in $[Ca^{2+}]_i$.
11. The absorption of intracellular dye at an isosbestic wavelength (585 nm), A_{585}, was computed from the optical transmission, T_{585}, measured both before and after injection of dye: $A_{585} = \log T_{585}$ (before) $- \log T_{585}$ (after). Changes in the absorption of intracellular dye induced by stimulation were calculated as follows. After the onset of a prolonged bright stimulus, the optical transmission at 660 nm, T_{660}, changes. The change of T_{660} is delayed with respect to the onset of the light (*10*). Therefore, we have calculated the change in absorption of the dye at 660 nm at time t_2, $\Delta A_{660}(t_2)$, by $\Delta A_{660}(t_2) = \log T_{660}(t_1) - \log T_{660}(t_2)$, where time t_1 was chosen to be as early as practical after the onset of the stimulus. Each complete scan of the diode array required 18 msec. The first scan was unusable because the stimulus light was turned on during this period. After the first scan, all the diodes in the array were read out and reset every 18 msec. Usually we took the second scan (which started at $t = 18$ msec) to be the reference scan for the calculation of ΔA_{660}.
12. J. E. Brown and J. R. Blinks, *J. Gen. Physiol.* **64**, 643 (1974).
13. The profiles of the change in absorbance at 660 nm across the cell do not change as a function of time as predicted by a simple diffusion model; the magnitude of the change declines faster at the maximum of the spatial profile than would be predicted by the magnitude of the broadening of the profile.
14. In previous studies, light-induced transients of intracellular arsenazo III were measured across large portions of *Limulus* ventral photoreceptors (*10*). Those recordings probably resulted from the fortuitous positioning of the measurement aperture over a region of the cell that contained a rhabdom. Also, light-induced transient increases of aequorin luminescence have been recorded from whole photoreceptors (*12*). Such spatially averaged luminescence records (in contrast to absorbance records) would be dominated by portions of the cell in which $[Ca^{2+}]_i$ increased most and influenced little by the much lower levels of luminescence arising from portions of the cell that had small changes in $[Ca^{2+}]_i$.
15. B. G. Calman and S. C. Chamberlain, *J. Gen. Physiol.* **80**, 839 (1982).
16. J. Stern, K. Chinn, J. Bacigalupo, J. Lisman, *ibid.*, p. 825.
17. A. Fein and J. S. Charlton, *ibid.* **66**, 823 (1975).
18. Supported by NIH grants EY 01914 and EY 01915. We thank S. R. Bolsover, J. A. Connor, U. B. Kaupp, J. E. Lisman, L. J. Rubin, and B. M. Salzberg for helpful comments on the manuscript.

11 August 1983; accepted 14 December 1983

Production of an Epidermal Growth Factor Receptor-Related Protein

Abstract. *Human epidermoid carcinoma A431 cells in culture produce a soluble 105-kilodalton protein which, by the criteria of epidermal growth factor (EGF) binding, recognition by monoclonal and polyclonal antibodies to the EGF receptor, amino-terminal sequence analysis and carbohydrate content, is related to the cell surface domain of the EGF receptor. The high rate of production and the finding that with biosynthetic labeling the specific activity of this 105-kilodalton protein exceeds that of the intact receptor indicate that it is not derived from membrane-bound mature receptor but is separately produced by the cell. These cells thus separately synthesize an EGF receptor that is inserted into the membrane and an EGF receptor-related protein that is secreted.*

The epidermal growth factor (EGF) receptor is a 170-kD membrane glycoprotein that contains intrinsic tyrosine kinase activity (*1, 2*). The EGF receptor has three functional domains: an EGF binding domain located on the external cell surface (*3, 4*), a transmembrane domain, and a cytoplasmic tyrosine kinase domain where adenosine triphosphate (ATP) is a donor for phosphorylation of intracellular substrates (*5, 6*). Binding of EGF to the receptor activates its tyrosine kinase activity which phosphorylates intracellular substrates (*6, 7*), increases ion fluxes (*8, 9*) and phosphatidyl inositol turnover (*10*), enhances receptor clustering and internalization of EGF receptor complexes (*3, 4*), and enhances receptor decay (*11*). The fate of internalized EGF receptors is not known, but there is evidence for sequestration in vesicles distinct from lysozymes (*12, 13*).

Using a monoclonal antibody to the EGF receptor, we have identified a 105-kD glycoprotein in medium from cultured human epidermoid carcinoma A431 cells. To characterize this extracellular EGF receptor-related protein (ERRP) we have studied EGF binding, recognition by several monoclonal and polyclonal antibodies to the EGF receptor, amino-terminal sequence homology with the EGF receptor, and carbohydrate content. Comparison of the rate of production and of the biosynthetic specific activity of this protein with those of the mature membrane bound EGF receptor indicates that ERRP is not a degradation product of the mature EGF receptor but is synthesized separately.

A431 cells produce a 105-kD protein that is specifically adsorbed to an immobilized monoclonal antibody to EGF receptor (termed 528). With time this 105-kD protein progressively accumulates in the medium of cultured $A431_8$ cells (Fig. 1A); the Coomassie blue stained bands correspond to the amount of protein produced on less than one 10-cm culture plate. The daily secretion rate was 0.4 μg of protein per 10^6 cells (Fig. 1A). Over this time period, cellular EGF receptor content remained constant. Like the EGF receptor, the ERRP was specifically bound to the monoclonal antibody and was not adsorbed to control columns containing immobilized mouse immunoglobulin G (IgG). Because the 528 monoclonal IgG used as an immunoabsorbent is a competitive inhibitor of EGF binding (*14, 15*), competitive elution with EGF was used to purify active EGF receptor–kinase protein (Fig. 1B). Likewise, the ERRP could be specifically eluted from the 528 IgG affinity column by EGF (Fig. 1B), an indication that it was also adsorbed via an EGF binding domain. Self-phosphorylation of the EGF receptor–kinase (*5*) was confirmed by incubating the washed column with [γ-^{32}P]ATP prior to elution of the protein. Under the same conditions, ERRP exhibited no detectable protein kinase activity (Fig. 1B). The absence of tyrosine kinase activity in the eluted ERRP was confirmed by means of a soluble assay with a synthetic peptide substrate (*16*). Also, ERRP was not phosphorylated by EGF receptor–kinase, suggesting that it also lacks the sites of self-phosphorylation present in the EGF receptor (data not shown).

Both the EGF receptor and ERRP stained well with the Schiff reagent (*17*), an indication that both are glycoproteins (Fig. 1C). Treatment of the EGF receptor protein with endoglycosidase F, which cleaves both high mannose glycans and complex glycans linked through asparagine (*18*), removes about 30 kD of oligosaccharide, leaving a 140-kD protein core (Fig. 1C). Treatment of ERRP with endoglycosidase F also removes a similar amount of oligosaccharide to produce an 80-kD protein core (Fig. 1C), suggesting that ERRP contains not only an EGF binding domain but that its glycosylation is similar to the EGF receptor protein. The protein doublet detected in samples treated with endoglycosidase F presumably arose during the prolonged incubation from a small proteolytic contamination present in the enzyme preparation (*18*).

To define further the relation of ERRP produced into the culture medium and the cell surface EGF receptor protein, we examined its interaction with several antibodies to the EGF receptor. ERRP competes with EGF receptor protein for binding to monoclonal antibody 29.1 (*19*) and to polyclonal antibodies to the EGF receptor. Monoclonal antibody 29.1 does